Folded phonons from lateral periodicity in (311) GaAs/AlAs corrugated superlattices

Z. V. Popović and M. B. Vukmirović
Institute of Physics, 11001 Belgrade, P.O. Box 57, Yugoslavia

Y. S. Raptis and E. Anastassakis
Physics Department, National Technical University, Zografou Campus, Athens 15780, Greece

R. Nötzel and K. Ploog
Paul-Drude-Institut für Festkörperelektronik, Hausvogteiplatz 5-7, D-10117 Berlin, Germany
(Received 27 April 1995)

We present an analysis of folded acoustic-phonon Raman scattering in (311)-oriented GaAs/AlAs superlattices with periodically corrugated interfaces. Besides folded phonons from q parallel to the growth direction, the folded acoustic-phonon modes from additional periodicity along the [01$\bar{1}$] direction are observed at frequencies that are in complete agreement with continuum model calculations. The influence of surface corrugation on confined optical-phonon modes is also discussed.

I. INTRODUCTION

The optical properties of GaAs/AlAs superlattices (SL's) and quantum wells, grown on substrates with non-(100) crystallographic orientations, have been studied extensively in the last few years.[1-3] It has been shown that high-quality superlattices can be grown by molecular-beam epitaxy (MBE) on practically any low-index crystallographic plane: (hkl), for $h,k,l = 0,1,2,3$. Special attention has been paid to (311)-oriented GaAs/AlAs superlattices due to their optical anisotropy,[4-7] connected with corrugation of this surface, with a lateral periodicity of 32 Å. The latter is revealed by reflection high-energy electron-diffraction (RHEED) measurements and high-resolution transmission-electron microscopy (TEM). It was shown[1] that there is a phase change in the surface corrugation during the growth of GaAs on AlAs and AlAs on GaAs, which gives rise to the formation of quantum-wire-like structures in GaAs/AlAs superlattices of this orientation (Fig. 1). There is some disagreement concerning the step height (10.2 Å[1] or 3.4 Å[2]). In Ref. 3

FIG. 1. Schematic representation of corrugation in a (311)-oriented GaAs$_{14}$AlAs$_{13}$ superlattice. The lateral periodicity is 32 Å, and the step height is 10 Å.

a sharp interface of superlattices with this orientation is reported. They concluded that surface corrugation is not an intrinsic effect of this orientation, and that arsenic deficiency during the growth process was most probably responsible for the observation of the interface corrugation in Ref. 1.

The vibrational properties of (311)-oriented GaAs/AlAs superlattices have been studied, and a comparison has been made between microscopic calculations, based on the shell model and phonon frequencies measured through Raman spectroscopy.[8] Optical-phonon modes have been studied for laser energies close to the band-edge resonance[9] and also close to higher-energy electronic transitions.[10] Near resonance with the SL band-edge, a splitting of each confined longitudinal-optical mode has been observed and ascribed to a finite in-plane wave vector induced by the lateral periodicity.[9] Close to resonance with the transition between the $n = 2$ electron and heavy-hole subbands, it was shown that an intraband deformation-potential mechanism contributes to the scattering intensity.[10]

The influence of interface corrugation on the vibrational properties of (311) GaAs/AlAs SL's was discussed in Refs. 11 and 12. It was shown there that the most important effects on the Raman-scattering spectra are (i) the appearance of peaks at frequencies higher than the TO$_{[01\bar{1}]}$ branch under crossed polarizations, and (ii) the shift of the peak of the first confined mode LO$_1$ toward lower frequencies. These effects are not observed in the Raman spectra of (311)-oriented GaAs/AlAs SL's presented in Ref. 12.

The Raman spectra for folded acoustic phonons in GaAs/AlAs SL's grown along the [311] direction are discussed in Refs. 13 and 14. Folded modes from all three acoustic branches are clearly observed at the same frequencies predicted by continuum model calculations. In Ref. 14 the appearance of the folded acoustic modes from lateral periodicity was discussed. Since the second-order LA doublet (for $q \| [311]$) appears at the position of the
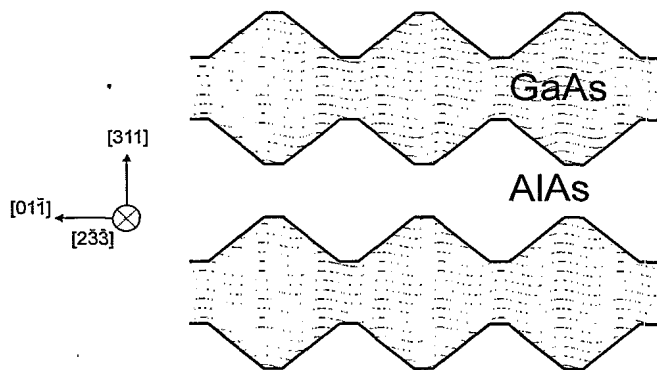
first LA doublet for $q \| [01\bar{1}]$, these modes were not resolved.[14]

In this work we present the analysis and Raman-scattering results for acoustic waves in (311)-oriented GaAs/AlAs SL's, which exhibit a wave-vector component $q_\perp$ in the SL plane (parallel to the $[01\bar{1}]$ direction). Raman selection rules are obtained for folded acoustic phonons consistent with lateral periodicity. The Raman spectra obtained for oblique scattering geometry show, in addition to the folded acoustic modes for $q_\| \| [311]$, the folded acoustic mode doublet which originates from lateral periodicity ($q_\perp \| [01\bar{1}]$). Furthermore, we have observed the frequency shift of the LO_1 mode, as well as the appearance of a mode in the Raman spectra under crossed polarizations, at frequencies higher than that of the $TO_{[01\bar{1}]}$ mode. These are strong indications of the presence of corrugation in the sample used.

II. PROPAGATION OF ACOUSTIC WAVES IN AN ARBITRARY DIRECTION

It is well known[15] that the propagation properties of acoustic waves in a superlattice can be obtained from the propagation of acoustic waves in the bulk materials. The analytic formulas relating the wave speed in a given direction with the elastic constants of the medium can be obtained from Christoffel's equation[16]

$$\det |c_{\lambda\mu\nu\rho} s_\mu s_\rho - \rho v^2 \delta_{\lambda\nu}| = 0 , \qquad (1)$$

where $c_{\lambda\mu\nu\rho} s_\lambda s_\rho$ is the Christoffel tensor, ρ is the mass density of the medium, v is the phase velocity, and $\delta_{\lambda\nu}$ is the Kronecker delta. s is the unit vector in the direction of propagation. If one of the eigenvectors is parallel to s, the corresponding acoustic wave is longitudinally polarized. Two other eigenvectors are perpendicular to s, and the acoustic waves associated with them are transverse. For a general direction of s the acoustic waves exhibit quasilongitudinal (QLA) and quasitransverse (QTA) polarizations. In cubic crystals (e.g., GaAs) there are only three directions of propagation ($\langle 100 \rangle$, $\langle 111 \rangle$, and $\langle 110 \rangle$) along which the acoustic waves are all purely longitudinal and purely transverse in character.[15]

In order to solve Eq. (1) for an arbitrary direction of s it is necessary that the stiffness constants c_{ij} be referred to a coordinate system x_1', x_2', x_3', of which the axis x_3' coincides with s. The transformation matrix which rotates the system of crystallographic axes x_1, x_2, x_3 to x_1', x_2', x_3' takes the form

$$R = \begin{vmatrix} l_1 & m_1 & n_1 \\ l_2 & m_2 & n_2 \\ l_3 & m_3 & n_3 \end{vmatrix} , \qquad (2)$$

where $l_\lambda, m_\lambda, n_\lambda$ ($\lambda = 1,2,3$) represent the direction cosines of x_λ' to relative to x_1, x_2, x_3, respectively.

The procedure for computing the rotated stiffness constants c_{ij}' is significantly simplified[17,18] by introducing a totally symmetric fourth-rank tensor with components $T_{\lambda\mu\nu\rho}$, which are easily constructed from the components of R [Eq. (1)].

$$T_{\lambda\mu\nu\rho} = l_\lambda l_\mu l_\nu l_\rho + m_\lambda m_\mu m_\nu m_\rho + n_\lambda n_\mu n_\nu n_\rho = T_{ij} = T_{ji} , \qquad (3)$$

where i and j are suppressed indices for $(\lambda\mu)$ and $(\nu\rho)$, respectively, i.e., Roman indices run from 1 to 6, whereas Greek indices run from 1 to 3. The components c_{ij}' are written as

$$c_{ij}' = c_{\lambda\mu\nu\rho}' = c_{\lambda\mu\nu\rho} + c(T_{\lambda\mu\nu\rho} - T_{\lambda\mu\nu\rho}^0) , \qquad (4)$$

where $c = c_{11} - c_{12} - 2c_{44}$ and $T_{ij}^0 = 1$ for $i = j = 1,2,3$, and zero otherwise.

Since $x_3' \| [l_3 m_3 n_3]$ is chosen along s, Eq. (1) takes the form

$$|c_{\lambda 3 \nu 3} - \rho v^2 \delta_{\lambda\nu}| = 0 ,$$

and the velocities of the sound waves in the arbitrary direction s of the cubic solid are determined by solving the secular equation

$$\begin{vmatrix} c_{55}' - \rho v^2 & c_{54}' & c_{53}' \\ c_{45}' & c_{44}' - \rho v^2 & c_{43}' \\ c_{35}' & c_{34}' & c_{33}' - \rho v^2 \end{vmatrix} = 0 , \qquad (5)$$

where c_{ij}' are calculated from Eq. (4).

Referring back to Fig. 1, where the (311) surface is shown schematically, the lateral periodicity of this structure appears along the $[01\bar{1}]$ direction. In order to calculate the frequencies of acoustic phonons which are folded because of lateral periodicity and propagate along the $[01\bar{1}]$ direction, we must consider the propagation of sound waves with $q_\perp \| [01\bar{1}]$. In this case the longitudinal waves turn out to be polarized along the [011] direction, and the transverse waves are polarized along two directions perpendicular to $[01\bar{1}]$. In the case of the $(01\bar{1})$ plane, shown in Fig. 2, there are several pairs of orthogo-
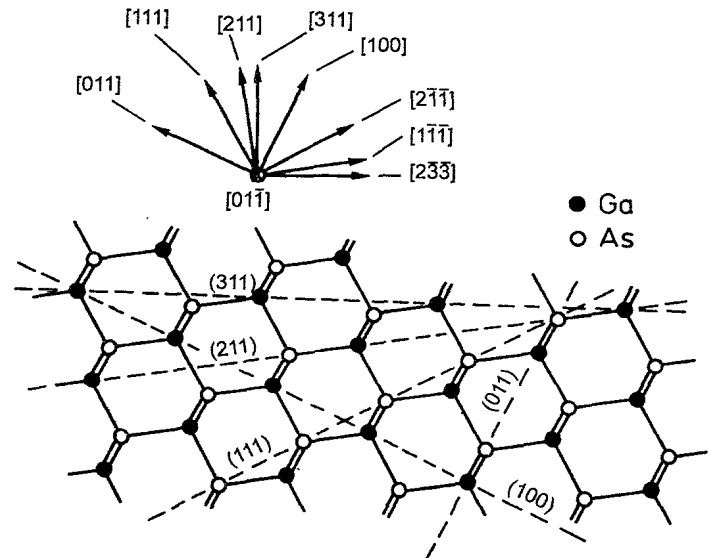

FIG. 2. Cross section of the GaAs crystal viewed along the $[01\bar{1}]$ direction. The (100), (011), (111), (211), and (311) planes are indicated by dashed lines.

TABLE I. System of right-handed orthogonal axes, secular equations, sound velocities, and Raman-scattering selection rules in the backscattering geometry for acoustic waves propagating along the $[01\bar{1}]$ direction ($q_{\perp}\|[01\bar{1}]$). c_{ij} are stiffness coefficients and a-h are the linear combinations of photoelastic coefficients p_{ij}: $a=\varepsilon_0^2(p_{11}+10p_{12}-2p_{44})/11$, $b=-3\varepsilon_0^2(p_{11}-p_{12}-2p_{44})/11\sqrt{2}$, $c=\varepsilon_0^2(9p_{11}+13p_{12}-18p_{44})/22$, $d=\varepsilon_0^2(p_{11}+5p_{12}-2p_{44})/6$, $e=-\varepsilon_0^2(p_{11}-p_{12}-2p_{44})/3\sqrt{2}$, $f=\varepsilon_0^2(p_{11}+2p_{12}-2p_{44})/3$, $g=\varepsilon_0^2(p_{11}+p_{12}-2p_{44})/2$, and $h=\varepsilon_0^2 p_{12}$.

$x_1'=[311]$ $\uparrow$ $x_3'=[01\bar{1}]\otimes\rightarrow x_2'=[2\bar{3}\bar{3}]$	$x_1'=[211]$ $\uparrow$ $x_3'=[01\bar{1}]\otimes\rightarrow x_2'=[1\bar{1}\bar{1}]$	$x_1'=[011]$ $\uparrow$ $x_3'=[01\bar{1}]\otimes\rightarrow x_2'=[100]$
$\begin{vmatrix} c_{44}+\dfrac{c}{11}-\rho v^2 & -\dfrac{3c}{11\sqrt{2}} & 0 \\ -\dfrac{3c}{11\sqrt{2}} & c_{44}+\dfrac{9c}{22}-\rho v^2 & 0 \\ 0 & 0 & c_{44}-\dfrac{c}{2}-\rho v^2 \end{vmatrix}$	$\begin{vmatrix} c_{44}+\dfrac{c}{6}-\rho v^2 & -\dfrac{c}{3\sqrt{2}} & 0 \\ -\dfrac{c}{3\sqrt{2}} & c_{44}+\dfrac{c}{3}-\rho v^2 & 0 \\ 0 & 0 & c_{44}-\dfrac{c}{2}-\rho v^2 \end{vmatrix}$	$\begin{vmatrix} c_{44}+\dfrac{c}{2}-\rho v^2 & 0 & 0 \\ 0 & c_{44}-\rho v^2 & 0 \\ 0 & 0 & c_{44}-\dfrac{c}{2}-\rho v^2 \end{vmatrix}$
$v_{LA}^{2[01\bar{1}]}=\dfrac{c_{11}+c_{12}+2c_{44}}{2\rho}$ $v_{QTA}^{2[311]}=\dfrac{c_{11}-c_{12}}{2\rho}$ $v_{QTA}^{2[2\bar{3}\bar{3}]}=\dfrac{c_{44}}{\rho}$	$v_{LA}^{2[01\bar{1}]}=\dfrac{c_{11}+c_{12}+2c_{44}}{2\rho}$ $v_{QTA}^{2[211]}=\dfrac{c_{11}-c_{12}}{2\rho}$ $v_{QTA}^{2[1\bar{1}\bar{1}]}=\dfrac{c_{44}}{\rho}$	$v_{LA}^{2[01\bar{1}]}=\dfrac{c_{11}+c_{12}+2c_{44}}{2\rho}$ $v_{TA}^{2[011]}=\dfrac{c_{11}-c_{12}}{2\rho}$ $v_{TA}^{[100]}=\dfrac{c_{44}}{\rho}$

Polarization	Scattering efficiency			Polarization	Scattering efficiency			Polarization	Scattering efficiency		
	$QTA^{[311]}$	$QTA^{[2\bar{3}\bar{3}]}$	$LA^{[01\bar{1}]}$		$QTA^{[211]}$	$QTA^{[1\bar{1}\bar{1}]}$	$LA^{[1\bar{1}\bar{1}]}$		$TA^{[011]}$	$TA^{[100]}$	$LA^{[01\bar{1}]}$
$x_1'x_1'$	0	0	a^2	$x_1'x_1'$	0	0	d^2	$x_1'x_1'$	0	0	g^2
$x_1'x_2'$	0	0	b^2	$x_1'x_2'$	0	0	e^2	$x_1'x_2'$	0	0	0
$x_2'x_2'$	0	0	c^2	$x_2'x_2'$	0	0	f^2	$x_2'x_2'$	0	0	h^2

nal directions along which the transverse waves could be polarized. Whether or not the waves are purely transverse along these directions will be decided only after solving the corresponding secular equation. We consider the following orthogonal set of directions: $[011],[100]$ and $[211],[1\bar{1}\bar{1}]$ (equivalent to $[111],[2\bar{1}\bar{1}]$ and $[311],[2\bar{3}\bar{3}]$). The sound velocities for all directions considered are collected in Table I. The first row of this table represents the system of axes, and the second row contains the corresponding secular equation [Eq. (5)]. The next row gives the corresponding sound velocities. Notice that in all four cases considered in Table I, the values of the corresponding velocities are the same. Fi-

nally, the Raman-scattering selection rules are given in the last row. These rules are obtained from the Brillouin tensor of bulk crystals, for $q_{\perp}\|[01\bar{1}]$. According to the selection rules given in Table I, only longitudinally polarized acoustic phonons, folded by lateral periodicity, are active in all cases shown in Table I for backscattering. Transverse and quasitransverse folded acoustic-phonon modes are not Raman active in backscattering. Thus we can only discuss longitudinal folded modes.

Continuum model calculations for acoustic waves, in the configuration described in the left column of Table I, are shown in Fig. 3(a) (the lateral periodicity is 32 Å). As can be seen from Fig. 3(a), the lateral periodicity folded
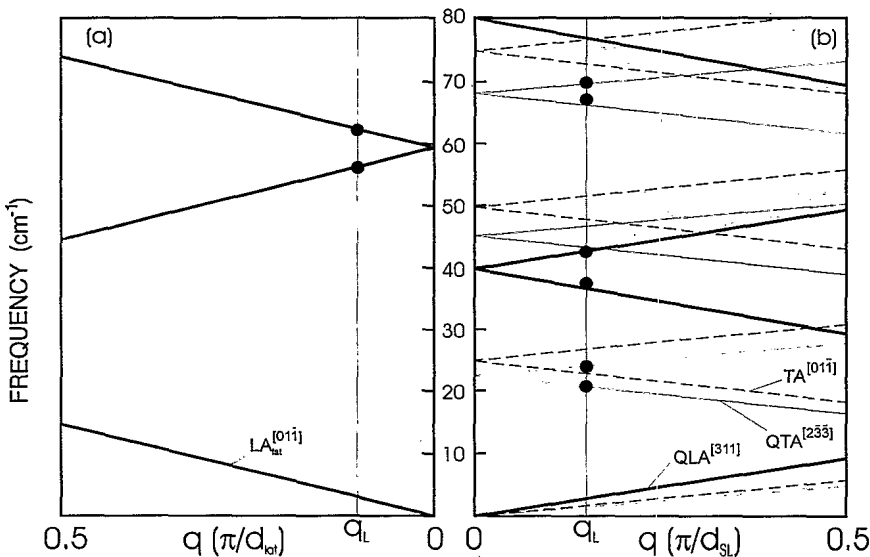

FIG. 3. Continuum model calculations for the (311) GaAs$_{14}$AlAs$_{13}$ superlattice with (a) a lateral periodicity $d=32$ Å, and (b) a superlattice periodicity of $d=46$ Å. Vertical lines are the laser line wave-vector positions. The points correspond to the observed modes measured at $T=300$ K with an excitation wavelength of 4880 Å.
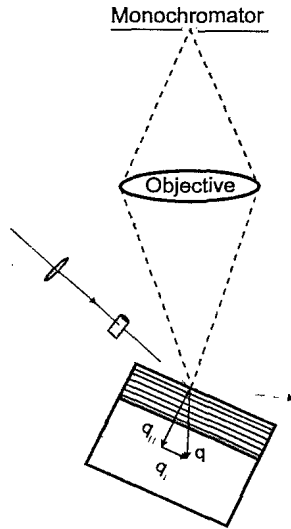
FIG. 4. Schematic view of the scattering geometry.

acoustic-phonon first-order doublet of longitudinal polarization (LA_{lat}) is centered at about 60 cm^{-1}. In order to observe this doublet it is necessary to use a SL sample which does not have any folded mode doublets at these frequencies. From all available samples, the best one was the sample with period $d=46$ Å ($d_{GaAs}=24$ Å, $d_{AlAs}=22$ Å). The continuum model calculation for this sample is presented in Fig. 3(b). Clearly, there are no first- or higher-order folded phonon doublets around 60 cm^{-1} for the (311) GaAs$_{14}$AlAs$_{13}$ superlattice for $q_{\parallel}$ parallel to the growth direction.

III. EXPERIMENT

We studied a short-period (311) GaAs$_{14}$AlAs$_{13}$ superlattice with a period of $d=46$ Å ($d_{GaAs}=24$ Å, $d_{AlAs}=22$ Å). The sample was grown by MBE on a (311)-oriented, undoped, semi-insulating GaAs substrate.

Details of the growth procedure and the x-ray characterization have been given earlier.[1,13] A schematic view of the scattering geometry is given in Fig. 4. A significant contribution of in-plane phonons ($q_\perp$) can be expected from this oblique scattering geometry. As an excitation source we used the 4880-Å line of an Ar-ion laser, focused on the sample through a cylindrical lens. The average power was about 500 mW. In order to increase the light flux on the sample, a collecting spherical lens was used in front of the cylindrical lens. The double monochromator used was a Jobin-Yvon model U 1000 with 1800 grooves/mm holographic gratings. The detector was a cooled RCA 31034 A photomultiplier with conventional photon-counting electronics.

IV. RESULTS AND DISCUSSION

The room-temperature Raman-scattering spectrum of the (311) GaAs$_{14}$AlAs$_{13}$ sample is shown in Fig. 5. The dominant structures in this spectrum are the first-order folded phonon doublets of quasitransverse (1QTA) and quasilongitudinal (1QLA) acoustic waves polarized along the [2$\bar{3}\bar{3}$] and [311] directions, respectively. These modes originate from superlattice periodicity along the growth direction (for $q_{\parallel}$). The frequencies of these doublets are in agreement with the continuum model calculation,[13] Fig. 3(b). In the 1QLA doublet there is one additional mode which we denote by ω_p. This is a laser plasma line, as checked by measuring the anti-Stokes spectrum. The properties of the first-order folded modes of this superlattice are discussed in more detail in a previously published paper,[13] and it will not be repeated here. As we mentioned above, the folded-phonon doublet from lateral periodicity could appear around 60 cm^{-1}. For this reason, we analyzed the spectral region between 50 and 75 cm^{-1} in more detail. The Raman spectrum in this region, shown in Fig. 5, is obtained by averaging 60 successive spectra. This multiscan procedure, which leads to an increase of the signal-to-noise ratio, was repeated several
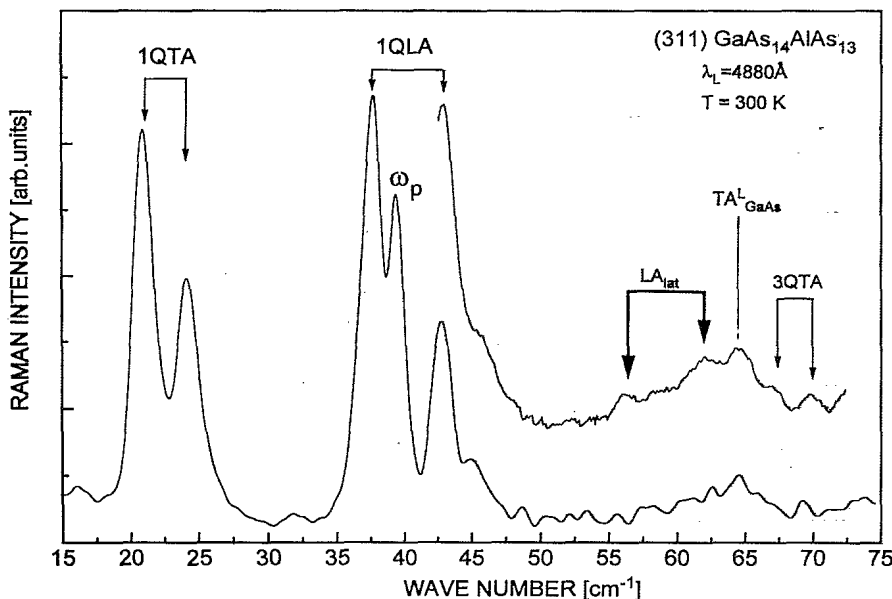

FIG. 5. Raman-scattering spectra of the (311) GaAs$_{14}$AlAs$_{13}$ superlattice measured at room temperature with the 4880-Å line of an Ar laser.

times on different places on the sample in order to check the assignment given in Fig. 5.

It can be seen from Fig. 5 that the dominant structure in the Raman spectrum in this spectral range is a broad peak around 64 cm^{-1}, which in fact is a superposition of this and two more modes centered at 56 and 62 cm^{-1}. Two additional low-intensity modes are resolved at about 67 and 70 cm^{-1}. The highest-intensity mode at 64 cm^{-1} is assigned to an L-point bulk mode because its frequency corresponds to the transverse-acoustic branch value of GaAs at the L point[19] (the zone-edge point in the [311] direction). This mode becomes Raman active due to imperfections on the surface and the scattering geometry used in this study (Fig. 4). The pair of modes centered at 68.5 cm^{-1} is assigned to a 3QTA doublet because its frequency is in agreement with the continuum model calculation. It is known[20] that for $a = d_{AlAs}/(d_{GaAs} + d_{AlAs})$ $= 0.46$, the intensity of the second-order doublet is negligible, but the third-order doublet is observable.

Finally, the two modes at about 56 and 62 cm^{-1} are assigned to a folded acoustic mode pair which originates from lateral periodicity according to the following two arguments: (i) no $q_\parallel$ mode exists for this superlattice, and (ii) the frequencies of these modes are in agreement with continuum model calculations for longitudinally polarized acoustic folded modes with $q_\perp \| [01\bar{1}]$. The frequencies of all modes discussed above are shown by full points in Fig. 3.

In Fig. 6, polarized Raman-scattering spectra at $T = 10$ K in the GaAs optical-phonon region are presented. We performed these measurements in order to check the influence of corrugation on the confined modes of this sample. As mentioned previously, surface corrugation causes the frequency of the LO_1 confined mode to shift to lower values and also leads to the appearance of modes for crossed polarizations at frequencies higher than that of the $TO^{[01\bar{1}]}$ mode.[12] Both these effects are present in the spectra of Fig. 6. That is, the LO_1-TO_1 splitting for this superlattice sample is calculated[8] to be 23.1 cm^{-1} without corrugation, and is actually observed to be somewhat lower (22.4 cm^{-1}). Second, the mode for crossed polarizations appears at about 277 cm^{-1} for this sample.

V. CONCLUSION

In conclusion, we have measured and analyzed the Raman-scattering spectra of the (311)-oriented GaAs$_{14}$AlAs$_{13}$ superlattice at room temperature in ob-
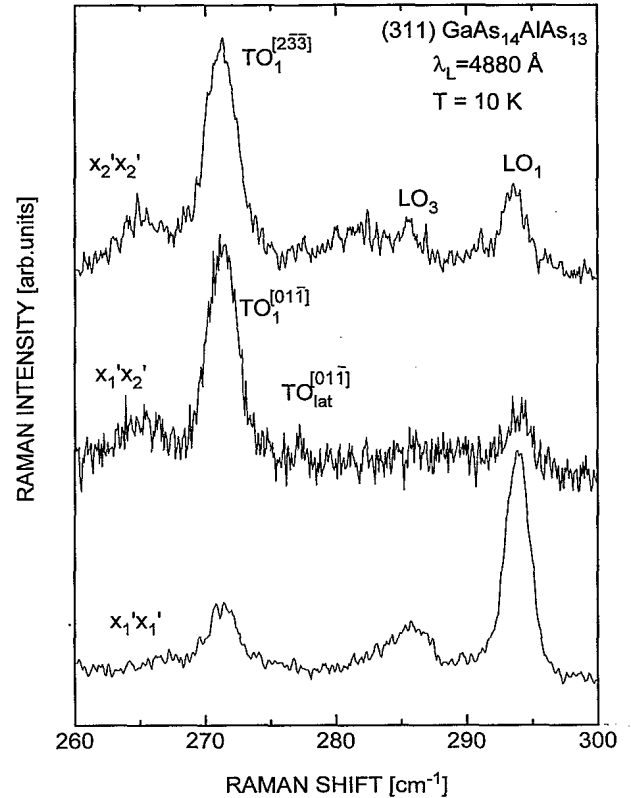

FIG. 6. Raman-scattering spectra of the (311) GaAs$_{14}$AlAs$_{13}$ superlattice for optical phonons, measured at 10 K for all three principal polarizations.

lique geometry. Besides folded acoustic phonon doublets associated with the superlattice periodicity for $q_\parallel \| [311]$ modes from lateral periodicity were also observed $(q_\perp \| [01\bar{1}])$. The influence of lateral periodicity is also observed in the confined optical-mode spectra which leads us to conclude that corrugation of (311) face is present and effective in the sample used.

ACKNOWLEDGMENTS

[1]R. Nötzel, L. Däweritz, and K. Ploog, Phys. Rev. B **46**, 4736 (1992).

[2]M. Wassermeier, J. Sudijono, M. D. Johnson, K. T. Leung, B. G. Orr, L. Däweritz, and K. Ploog, Phys. Rev. B **51**, 14 721 (1995).

[3]Y. Hsu, W. I. Wang, and T. S. Kuan, Phys. Rev. B **50**, 4973 (1994).

[4]Z. Ikonić, G. P. Srivastava, and J. C. Inkson, Phys. Rev. B **49**, 10 749 (1994).

[5]D. S. Jiang, X. Q. Zhou, M. Oestreich, W. W. Ruhle, R. Nötzel, and K. Ploog, Phys. Rev. B **49**, 10 786 (1994).

[6]G. Armelles, P. Castrillo, P. S. Dominguez, L. Gonzalez, R. Ruiz, D. A. Contreras-Solorio, V. R. Velesco, and F. Garcia Moliner, Phys. Rev. B **49**, 14 020 (1994).

[7]J. Jouanin, A. Hallaoui, and D. Bertho, Phys. Rev. B **50**, 1645 (1994).

[8]Z. V. Popović, E. Richter, J. Spitzer, M. Cardona, J. A. Shields, R. Nötzel, and K. Ploog, Phys. Rev. B **49**, 7577

(1994).

[9] J. A. Shields, R. Nötzel, M. Cardona, L. Däweritz, and K. Ploog, Appl. Phys. Lett. **60**, 2537 (1992).

[10] J. A. Shields, Z. V. Popović, M. Cardona, J. Spitzer, R. Nötzel, and K. Ploog, Phys. Rev. B **49**, 7584 (1994).

[11] P. Castrillo, L. Colombo, and G. Armelles, Phys. Rev. B **49**, 10 362 (1994).

[12] P. Castrillo, G. Armelles, L. Gonzalez, P. S. Dominguez, and L. Colombo, Phys. Rev. B **51**, 1647 (1995).

[13] Z. V. Popović, J. Spitzer, T. Ruf, M. Cardona, R. Nötzel, and K. Ploog, Phys. Rev. B **48**, 1659 (1993).

[14] M. V. Belousov, V. Yu. Davydov, I. E. Kozin, P. S. Kop'ev, and N. N. Ledentsov, Pis'ma Zh. Eksp. Teor. Fiz. **57**, 112

(1993) [JETP Lett. **57**, 120 (1993)].

[15] Z. V. Popović, J. H. Trodhal, M. Cardona, E. Richter, D. Strauch, and K. Ploog, Phys. Rev. B **40**, 1202 (1989).

[16] J. Sapriel, *Acousto-Optics* (Wiley, New York, 1989), p. 18.

[17] E. Anastassakis, J. Cryst. Growth **114**, 647 (1991).

[18] E. Anastassakis and E. Liarokapis, Phys. Status Solidi B **149**, K1 (1988).

[19] D. Strauch and B. Dorner, J. Phys. Condens. Matter **2**, 1457 (1990).

[20] B. Jusserand and M.Cardona, in *Light Scattering in Solids V*, edited by G. Güntherodt and M. Cardona (Springer, Heidelberg, 1989), p. 49.